ARTHRITIS & RHEUMATISM
Vol. 62, No.7, July 2010, pp 2013–2022
DOI 10.1002/art.27486

Endothelial Nitric Oxide Synthase Deficiency in Mice Results in Reduced Chondrocyte Proliferation and Endochondral Bone Growth

Qian Yan, Qingping Feng, and Frank Beier

Objective. **Nitric oxide (NO) and aberrant chondrocyte differentiation have both been implicated in the pathogenesis of osteoarthritis, but whether these processes are connected is unknown, and the role of specific NO synthase (NOS) enzymes in chondrocyte physiology is unclear. This study was undertaken to examine the effects of inactivation of endothelial cell NOS (eNOS) on cartilage development in mice.**

Methods. **Skeletal growth and development of mice carrying a null mutation in the *eNOS* gene was compared with that of their control littermates. In situ analyses were complemented by experiments with primary chondrocytes and tibial explants from these mice.**

Results. **Mice that were deficient in *eNOS* showed increased fatality and reduced bone growth, with hypocellular growth plates and a marked reduction in the number of proliferating chondrocytes. In vitro studies demonstrated lower chondrocyte numbers and reduced endochondral bone growth in mutant mice, suggesting that the role of eNOS signaling in chondrocyte proliferation is cell autonomous. Reduced chondrocyte numbers appear to be caused by decreased cyclin D1 and increased p57 expression in mutant mice, resulting in slower cell cycle progression and earlier cell cycle exit. In addition, expression of early chondrocyte markers such as SOX9 was reduced, and prehypertrophic markers were expressed prematurely in mutant mice.**

Conclusion. **Our findings identify a novel and important role of eNOS in chondrocyte proliferation and endochondral bone growth and demonstrate that loss of eNOS results in premature cell cycle exit and prehypertrophic chondrocyte differentiation during cartilage development.**

Nitric oxide (NO) plays an important role in the progression of osteoarthritis (OA), in part by influencing the physiology of chondrocytes (1,2). NO is synthesized through L-arginine by NO synthases (NOS) in many cell types. Three different types of NOS have been identified. The neuronal NOS (nNOS or NOS1) and endothelial NOS (eNOS or NOS3) forms are constitutively expressed, and their activity is regulated by intracellular signaling and the calcium-binding protein calmodulin (3). The inducible form (iNOS or NOS2) is stimulated at the level of expression by factors including lipopolysaccharide and cytokines, such as interleukin-1, tumor necrosis factor α, and interferon-α, and leads to sustained and high levels of NO, mainly in inflammatory disease (1,2,4).

Changes in the articular chondrocyte phenotype, such as initiation of hypertrophic differentiation, are thought to play an important role in the pathogenesis of OA (5–7). Physiologically, chondrocyte hypertrophy occurs in the process of endochondral ossification that gives rise to most bones in the vertebrate skeleton, such as the long bones of the limbs (8,9). Endochondral ossification involves the formation of a highly controlled and precisely shaped cartilage template that is subsequently replaced by bone tissue and bone marrow (10). Once mesenchymal cells commit to the chondrogenic lineage, the subsequent events of endochondral bone formation occur through the epiphyseal growth plate (11), which consists of zones of resting, proliferating, and hypertrophic chondrocytes organized in distinguishable columnar arrays (10). Within the growth plate, proliferation of chondrocytes occurs in a unidirectional

Supported by the Canadian Institutes of Health Research (CIHR grant 3152A01). Dr. Beier is recipient of a Canada Research Chair in Musculoskeletal Health at the Schulich School of Medicine and Dentistry, University of Western Ontario.

Qian Yan, MSc, Qingping Feng, PhD, Frank Beier, PhD: University of Western Ontario, London, Ontario, Canada.

Address correspondence and reprint requests to Frank Beier, PhD, Department of Physiology and Pharmacology, Schulich School of Medicine and Dentistry, University of Western Ontario, London, Ontario N6A 5C1, Canada. E-mail: fbeier@uwo.ca.

Submitted for publication December 18, 2009; accepted in revised form March 25, 2010.

manner, resulting in longitudinal bone growth (12,13). After exiting the cell cycle, chondrocytes start to differentiate into prehypertrophic and eventually hypertrophic chondrocytes (14–16). Hypertrophic chondrocytes direct mineralization of the surrounding extracellular matrix, attract blood vessel invasion, and ultimately undergo apoptosis while being replaced by bone and bone marrow (13,17). Proliferation and hypertrophy of growth plate chondrocytes and extracellular matrix production drive the longitudinal growth of endochondral bones and eventually determine body length in mammals (13,18).

Since both NO signaling and altered chondrocyte differentiation contribute to OA, it is important to examine whether both processes are connected. Studies in the chicken suggest that NO signaling promotes chondrocyte hypertrophy (19,20), but the roles of NO and in particular the individual *NOS* genes in mammalian cartilage development are not well understood. In this study, we used a genetic approach to address the role of eNOS in chondrocyte differentiation and endochondral ossification in vivo. Inactivation of the *eNOS* gene resulted in a number of phenotypes, including reduced proliferation and earlier cell cycle exit of chondrocytes. Overall, these data provide novel information regarding the importance of eNOS/NO signaling in chondrocyte development and identify downstream regulators of endochondral ossification.

MATERIALS AND METHODS

Animals and materials. Pregnant CD1 mice were purchased from Charles River. Cell culture materials and general chemicals were obtained from Invitrogen, Sigma, or VWR unless otherwise stated. The following antibodies were used in this study: $p57^{Kip2}$ (catalog no. sc8298; rabbit antibody against human protein), retinoic acid–related orphan receptor α (RORα) (catalog no. sc28612; rabbit antibody against human protein), activating transcription factor 3 (ATF-3) (catalog no. sc188; rabbit antibody against human protein), goat anti-mouse (catalog no. sc2005), goat anti-rabbit (catalog no. sc2004) (all from Santa Cruz Biotechnology); cyclin D1 (SP4; rabbit antibody against human, mouse, and rat proteins) (catalog no. #9104-S1; NeoMarkers); proliferating cell nuclear antigen (PCNA; mouse antibody against human, mouse, and rat proteins) (catalog no. 2586; Cell Signaling Technology); hypoxia-inducible factor 1α (HIF-1α; rabbit antibody against human protein) (catalog no. 07-628; Upstate Biotechnology); and bromodeoxyuridine (BrdU; mouse antibody, species-independent) (catalog no. 03-3900; Zymed).

Mouse breeding and genotyping. Mice with a deletion of the *eNOS* gene (stock no. 2684) (21) and control mice on the C57BL/6 background were obtained from The Jackson Laboratory. Mice were kept under 12-hour light/12-hour dark conditions, and fed tap water and regular chow ad libitum. All procedures involving animals were approved by the University of Western Ontario Animal Care and Use Committee. All experiments were done using crosses of heterozygous mice to compare knockout animals with wild-type controls within the same litter. For polymerase chain reaction (PCR) genotyping, tail snips were used to prepare DNA for PCR analysis. PCR genotyping was performed by simultaneous amplification of the *eNOS* wild-type and null alleles as previously described (22). PCR fragments were analyzed by agarose gel electrophoresis.

Skeletal staining and histology. Animals were skinned, eviscerated, and dehydrated in 95% ethanol overnight and then in acetone overnight. Skeletons were stained with 0.015% Alcian blue, 0.05% alizarin red, and 5% acetic acid in 70% ethanol for several days. Skeletons were then cleared in 1% KOH, passed through descending concentrations of KOH, and stored in glycerol/ethanol (1:1) (23,24). After dissection of mice, bones were rinsed with phosphate buffered saline, fixed in 4% paraformaldehyde overnight, placed in 10% formalin solution, and sent to the Molecular Pathology Core Facility at the Robarts Research Institute (London, Ontario, Canada) for embedding and sectioning into 4-μm sections. After sectioning, bones were stained with hematoxylin and eosin or Safranin O–fast green using standard protocols (23–25) or used for immunohistochemistry as described below.

Immunohistochemistry and BrdU labeling. For immunohistochemistry, sections unstained prior to use were incubated in 3% H_2O_2 for 15 minutes at room temperature, boiled for 20 minutes in 10 m*M* sodium citrate (pH 6.0), and blocked with 5% goat serum at room temperature for 30 minutes. Sections were incubated with primary antibody overnight at 4°C and secondary antibodies according to the recommendations of the manufacturers. After washing, the sections were incubated for 1–10 minutes with diaminobenzidine substrate solution (Dako), washed, and mounted. All images were taken at room temperature with a Retiga EX camera connected to a Leica DMRA2 microscope using OpenLab software, version 4.0.4. For cell counts in sections, all cells and cells positive for staining with primary antibody labeling were counted from 3 different areas of 1 section. Sections from at least 3 mice per genotype, and at least 3 sections from every mouse, were analyzed, and the mean and SD from all counts per genotype are shown.

For BrdU labeling, newborn mice were injected intraperitoneally with BrdU (Roche) at a dose of 0.03 mg/gm of body weight 1 hour before mice were killed. BrdU was detected in paraffin sections using anti-BrdU antibody as described above. For all antibodies, negative controls were used following the same protocol in the absence of the primary antibody.

Primary cell culture and MTT assays. Tibiae, femurs, and humeri were isolated from knockout and control mice on embryonic day 15.5 (E15.5) using a Stemi DV4 stereo microscope (Zeiss). Twenty bones from the same genotype were placed in 2 ml of α-minimum essential medium (α-MEM; Invitrogen)/well containing 0.2% bovine serum albumin (BSA), 1 m*M* β-glycerophosphate, 0.05 mg/ml ascorbic acid, and penicillin/streptomycin in a 6-well culture dish (Falcon), as previously described (26). Then medium was removed, and every 10–12 bones from each group were placed in 1 ml of 0.25% trypsin-EDTA (Invitrogen) for 15 minutes at 37°C.

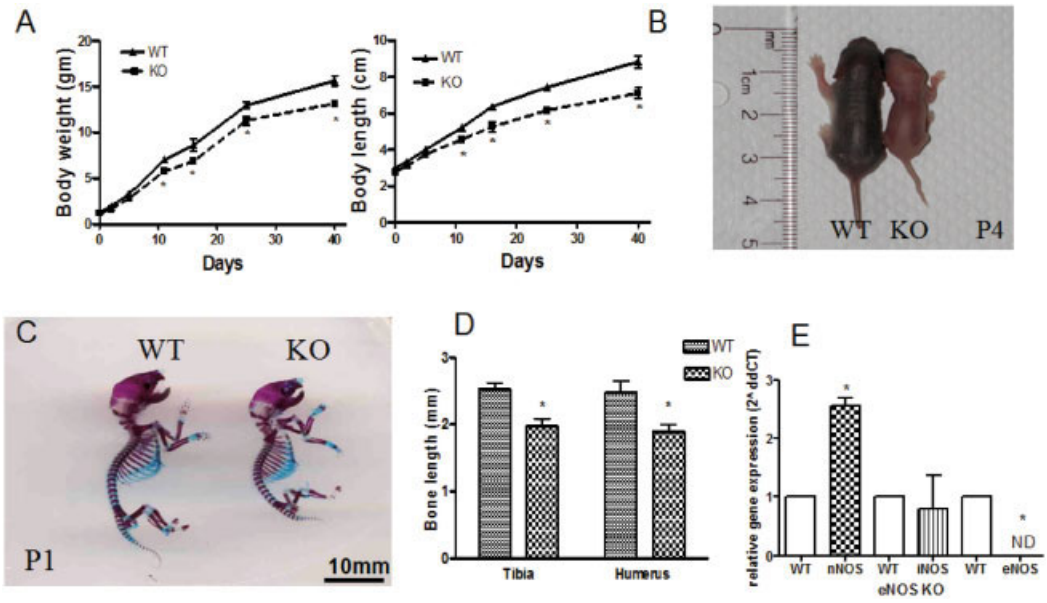

Figure 1. Reduced growth upon loss of endothelial nitric oxide synthase (eNOS). Body weight and body length of mice were determined during the first 42 days of life. **A,** Slower increases in both body weight and body length in *eNOS*-deficient (knockout [KO]) mice compared with their wild-type (WT) littermates. Values are the mean ± SD (n ≥ 8 mice per genotype). * = $P < 0.05$. **B,** Comparison of an *eNOS*-knockout mouse with a wild-type littermate on postnatal day 4 (P4), demonstrating a delay in growth and development and a kinky tail in the mutant mouse. **C,** Whole skeletal staining with Alcian blue and alizarin red on postnatal day 1, showing no morphologic difference other than reduced size in the mutant mouse. **D,** Measurements of selected individual bones, confirming reduced bone length in humeri and tibiae in neonatal mutant mice. **E,** Results of real-time reverse transcriptase–polymerase chain reaction using RNA extracted directly from neonate cartilage from *eNOS*-knockout mice. Transcript levels for neuronal NOS (nNOS) were up-regulated, inducible NOS (iNOS) mRNA levels did not change, and eNOS transcripts were not detectable (ND) in knockout mice. Bars in **D** and **E** show the mean and SD (n = 4 mice per group). * = $P < 0.05$ versus wild-type mice.

Trypsin was subsequently replaced with 1 mg/ml of collagenase P (Roche) in Dulbecco's modified Eagle's medium (DMEM)/10% fetal bovine serum (FBS; Invitrogen), and cells were incubated at 37°C with rotation at 100 revolutions per minute for 90 minutes. Following digestion, the cell suspension was centrifuged for 5 minutes at 1,000 rpm, and the collagenase-containing supernatant was decanted. Chondrocytes were resuspended in media containing a 2:3 ratio of DMEM to F12, 10% FBS, 0.5 m*M* L-glutamine, and penicillin/streptomycin (25 units/ml) supplemented with 0.25 m*M* ascorbic acid (Sigma) and 1 m*M* β-glycerophosphate (Sigma). Chondrocytes (10,000 cells/ml) were seeded in a 96-well culture dish (Falcon) containing 100 μl of medium per well and cultured in the presence of 5% CO_2. Cell numbers were determined by MTT assay as previously described (27,28).

Organ culture. Tibiae were isolated from E15.5 embryos from wild-type and knockout mice as described above (29,30). Dissection day was considered to be day 0, and tibiae (1/well) were allowed to recover from dissection overnight in serum-free α-MEM media (1 ml/well) containing 0.2% BSA, 0.5 m*M* L-glutamine, 40 units of penicillin/ml, and 40 μg of streptomycin/ml in 24-well Falcon plates, as previously described (29,30). All culture dishes were maintained in an incubator containing 5% CO_2. The next morning, bone length was measured using an eyepiece in the Stemi DV4 stereo microscope. Media were changed every 48 hours beginning on day 1, and bones were measured on days 2, 4, and 6. Results are expressed as growth in length relative to day 1. Experiments were performed at least 3 times, using 4–6 bones per treatment for each trial.

Western blotting. Fresh cartilage from the limbs of newborn mice was dissected in cold Puck's solution A (80 gm/liter NaCl, 4.0 gm/liter KCl, 0.6 gm/liter KH_2PO_4, 0.9 gm/liter $Na_2HPO_4 \cdot 7H_2O$, and 10 gm/liter glucose [pH 7.4]). Modified radioimmunoprecipitation buffer extracts of cartilage were used directly for Western blotting (5,23,24). Blocking, incubation with antibodies, and washing were carried out according to the recommendations of the supplier of the primary antibody. Immunoblots were developed using the ECL detection system (Amersham). Blots shown in the figures are representative blots from 3 independent littermate comparisons.

RNA isolation and real-time reverse transcriptase–PCR (RT-PCR). Total RNA was isolated from the epiphyseal cartilage of long bone from newborn mice using TRIzol, according to the recommendations of the manufacturer (Invitrogen). TaqMan real-time PCR was performed as previously described (26,31) using primers and probe sets from Applied

Biosystems (for *Sox9*, Mm00448840_m1; for *Col2a*, Mm00491889_m1; for *Col10a*, Mm00487041_m1; for *Rora*, Mm00443103_m1; for *Hif1a*, Mm00468869_m1; for *Nos1*, Mm00435175_m1; for *Nos2*, Mm00440485_m1; for *Nos3*, Mm00435204_m1; for *Gapdh*, Mm99999915_g1). Data were normalized to GAPDH messenger RNA (mRNA) levels and represent the mean and SD from direct comparisons of mutant and control littermates from 3 different crosses. Statistical significance of real-time PCR results was determined by one-way analysis of variance (ANOVA) with Bonferroni post-test using GraphPad Prism, version 4.00 for Windows (GraphPad Software).

Statistical analysis. All experiments were performed with at least 3 independent litters. Statistical significance was determined by a one-way ANOVA with Bonferroni post-test using GraphPad Prism, version 4.00 for Windows.

RESULTS

Reduced viability and growth in *eNOS*-knockout mice. We used *eNOS*-deficient mice to address the role of this gene in cartilage development in vivo. Based on our breeding protocol using heterozygous mice, Mendelian ratio would predict that 50% of the newborn mice would be heterozygous and 25% would be homozygous *eNOS*-null mice. However, examination of genotype distribution in the newborn mice revealed that only 14% of the mice were homozygous for the mutant *eNOS* allele, and 40% were heterozygous. Analyses of genotypes at different embryonic stages showed the expected Mendelian distribution (data not shown). These data suggest that loss of the *eNOS* gene results in increased embryonic death at the late prenatal or perinatal stage. Additionally, 44% of the newborn $eNOS^{-/-}$ mice died shortly after birth. Slightly decreased body weight (86%) and length (92%) were found in $eNOS^{-/-}$ mice at birth. Analysis of both parameters over the first 42 days of life demonstrated that growth retardation became more pronounced in surviving $eNOS^{-/-}$ mice as the animals aged (Figure 1A). Growth retardation was similar in female and male mice (data not shown). However, some of the $eNOS^{-/-}$ mice demonstrated a more severe delay in growth and development, and some were born with a kinky tail (6 of 20 knockout mice from 9 litters) (Figure 1B).

We next examined the skeletal phenotype of *eNOS*-deficient mice. Whole skeletal staining with Alcian blue and alizarin red confirmed that mutant mice had a smaller skeleton than control littermates on postnatal day 1 (Figure 1C). The majority of mutant mice showed no obvious morphologic changes in the skeleton. Detailed observation of the whole skeleton of mutant mice revealed a smaller rib cage and skull and a shorter appendicular skeleton. Measurement of selected

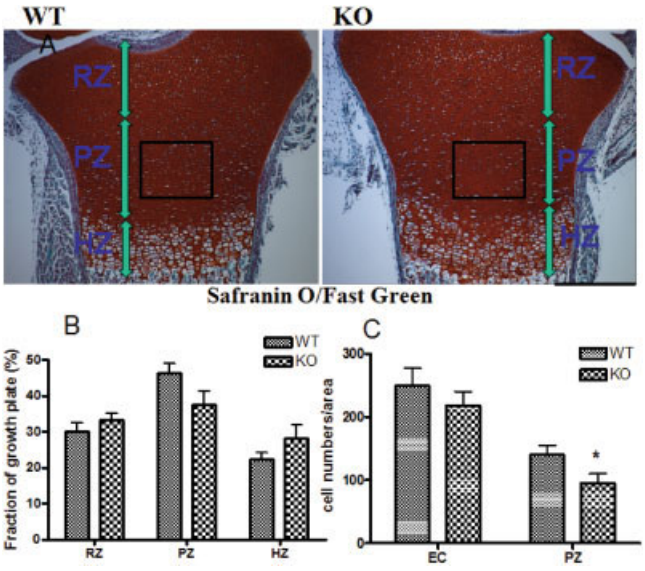

Figure 2. Reduced proliferating chondrocyte numbers in mutant growth plates. **A,** Histologic analyses demonstrating that growth plates from newborn mutant mice display a similar arrangement of chondrocytes into the proliferative zone (PZ) and hypertrophic zone (HZ) as control mice. Boxed areas show the areas in which proliferating cells were counted. Bar = 500 μm. **B,** Length of the resting zone (RZ), proliferative zone, and hypertrophic zone in the growth plates. There were no significant changes in mutant mice. **C,** Cell numbers per area in the epiphyseal cartilage (EC) and proliferative zone. Cell numbers in the proliferative zone of the growth plate in mutant mice were lower (71%). Bars in **B** and **C** show the mean and SD ($n \geq 8$ mice per genotype). $* = P < 0.05$ versus wild-type mice. See Figure 1 for other definitions.

individual bones confirmed reduced bone length of humeri (76%) and tibiae (80%) in neonatal mutant mice (Figure 1D). Real-time RT-PCR using RNA extracted directly from neonate cartilage from *eNOS*-knockout mice demonstrated up-regulated nNOS transcript levels compared with wild-type controls. Levels of mRNA for iNOS were unchanged, and eNOS transcripts could not be detected in mutant mice, as expected (Figure 1E).

Reduction of chondrocyte proliferation in the mutant growth plate. To elucidate the cellular basis of the reduced skeletal growth, we analyzed growth plate organization. Growth plates from newborn mutant mice displayed a chondrocyte arrangement in proliferative and hypertrophic zones similar to that in control animals (Figure 2A). Measurement of the length of the various growth plate zones showed that the proliferative zone was slightly smaller and the hypertrophic zone was slightly larger in knockout growth plates, but these differences were not statistically significant (Figure 2B). The $eNOS^{-/-}$ growth plates were hypocellular, espe-

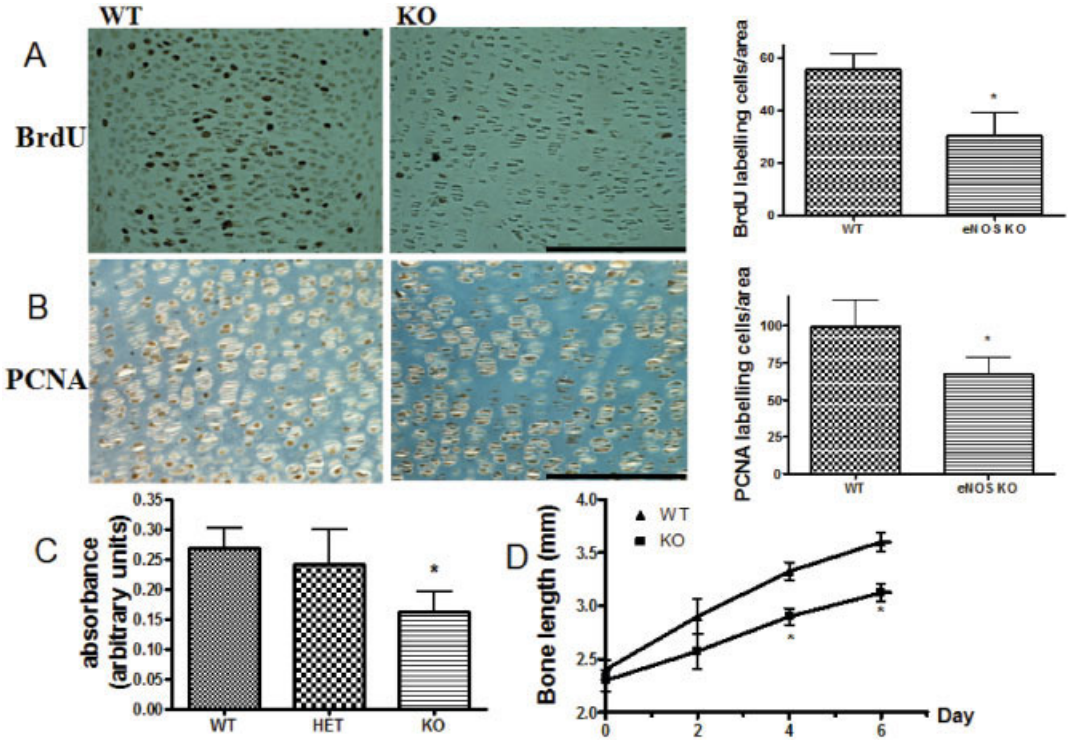

Figure 3. Reduction in chondrocyte proliferation and endochondral bone growth in vitro upon loss of *eNOS*. **A,** Marked reduction in replicating cells in *eNOS*-knockout mice, shown by bromodeoxyuridine (BrdU) incorporation assays and confirmed by counting of labeled cells. Bar = 200 μm. **B,** Reduced numbers of positive cells per area in *eNOS*-knockout mice, shown by immunohistologic staining of proliferating cell nuclear antigen (PCNA). **C,** Numbers of primary chondrocytes in wild-type, heterozygous (HET), and $eNOS^{-/-}$ mice. MTT assays demonstrated a slower increase in numbers of primary chondrocytes in $eNOS^{-/-}$ mice than in their wild-type or heterozygous littermates. **D,** Reduced bone growth in tibiae from mutant mice compared with those from control animals on days 4 and 6 of organ culture. Values are the mean ± SD (n ≥ 4 mice per genotype). $* = P < 0.05$ versus wild-type mice. See Figure 1 for other definitions.

cially in the center of the growth plates (Figure 2A). Counts of cell numbers in the proliferative zone of the growth plate revealed fewer cells per area in mutant mice (71% of control cell numbers), while cell counts in the epiphyseal cartilage did not show a significant difference between genotypes (Figure 2C). Analyses of additional long bones at different developmental stages confirmed that reduced numbers of cells in the proliferative zone are a general feature of $eNOS^{-/-}$ bones (data not shown).

We next investigated whether changes in cell proliferation are the cause of hypocellularity in *eNOS*-deficient growth plates. BrdU incorporation assays showed a marked reduction in replicating cells in mutant mice that was confirmed by cell counts (Figure 3A). Control experiments in these and all subsequent immunohistochemistry studies were done without primary antibody and showed no staining (results not shown). Immunohistochemical staining for PCNA demonstrated a similar reduction in the number of positive cells in mutant mice (Figure 3B). These findings demonstrate that the proliferation of chondrocytes is reduced upon loss of *eNOS*.

Because the mutant mice used in this study were *eNOS*-deficient in all cells of the body, it was possible that reduced bone growth and chondrocyte proliferation were secondary to loss of eNOS in other cell types. We therefore compared proliferation of primary chondrocytes from control and $eNOS^{-/-}$ mice in culture. MTT assays demonstrated that cells in mutant mice increased their numbers more slowly than those in control littermates, while chondrocytes from heterozygous mice did not show any differences from wild-type cells (Figure 3C). In addition, we conducted organ culture experiments by growing tibiae from E15.5 $eNOS^{-/-}$ and wild-type mice in culture for 6 days. While bones from

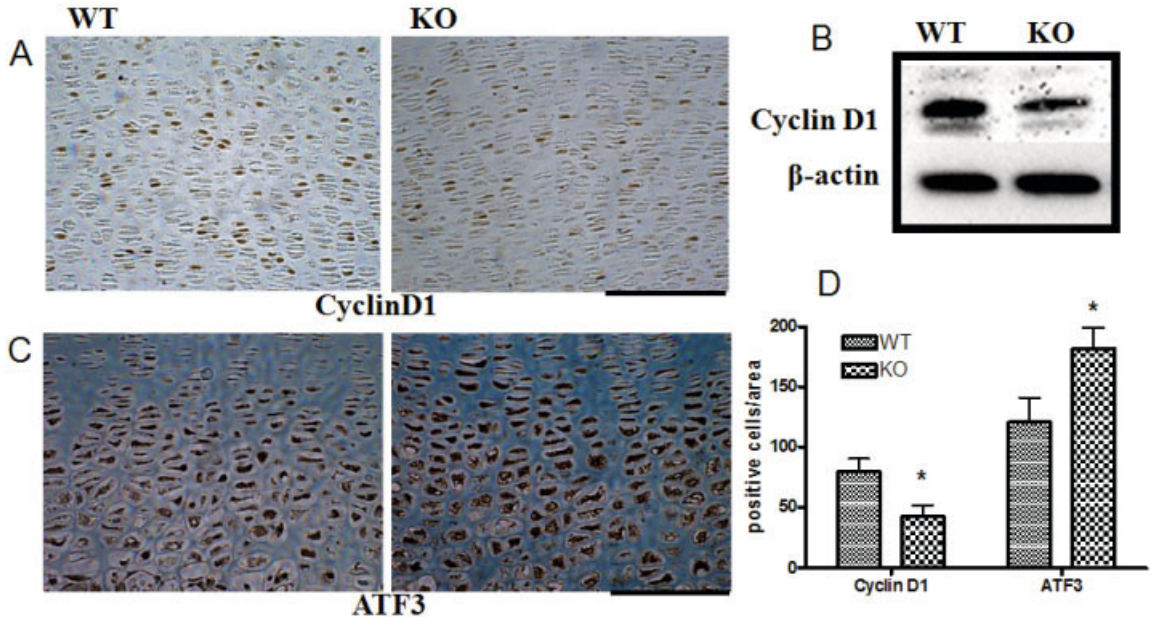

Figure 4. Reduced cyclin D1 expression in *eNOS*-deficient mice. **A,** Immunohistochemical staining for cyclin D1, showing reduced numbers of positive cells in *eNOS*-knockout mice. **B**, Western blot confirming reduced cyclin D1 expression in knockout mice. **C,** Immunohistochemical staining showing that activating transcription factor 3 (ATF-3) was up-regulated in *eNOS*-knockout mice. **D**, Numbers of cyclin D1–positive and ATF-3–positive cells per area. Cell numbers confirmed the changes in the knockout mice. Bars in **A** and **C** = 200 μm. Representative results from at least 4 independent experiments are shown. Bars in **D** show the mean and SD. $* = P < 0.05$ versus wild-type mice. See Figure 1 for other definitions.

both genotypes were of similar length at the beginning of the culture, bones from mutant mice showed significantly reduced growth compared with those from control animals on days 4 and 6 (Figure 3D). These data suggest that eNOS is required for normal chondrocyte proliferation and endochondral bone growth in a cell-autonomous manner.

Reduced cyclin D1 expression in *eNOS*-deficient mice. To elucidate the reason for reduced cell numbers in $eNOS^{-/-}$ mice, we examined cell cycle protein expression in growth plates. Immunohistochemical staining of cyclin D1, which is required for normal chondrocyte proliferation (32,33), demonstrated reduced numbers of positive cells in mutant mice (Figure 4A). Reduced cyclin D1 protein expression in *eNOS*-deficient cartilage was confirmed by Western blotting (Figure 4B). We recently demonstrated that the transcription factor ATF-3 is up-regulated during chondrocyte hypertrophy and represses the activity of the cyclin D1 promoter in chondrocytes (34). Immunohistochemistry demonstrated increased ATF-3 expression in *eNOS*-deficient growth plates (Figure 4C), suggesting that premature induction of ATF-3 expression in mutant mice leads to repression of cyclin D1 transcription and chondrocyte proliferation.

Premature differentiation of *eNOS*-deficient chondrocytes. Since reduced chondrocyte proliferation is often associated with premature cell cycle exit and maturation (32), we examined the expression of additional markers of prehypertrophic chondrocytes. Immunohistochemistry and Western blotting revealed increased expression of the cell cycle inhibitor p57, which promotes cell cycle exit and is required for normal chondrocyte differentiation, in mutant mice (Figures 5A and B). In wild-type growth plates, p57 protein was restricted to a small band of prehypertrophic chondrocytes, while in knockout growth plates, there was both earlier staining in late proliferative cells and sustained staining in hypertrophic chondrocytes. The nuclear receptor RORα is another marker for prehypertrophic and hypertrophic chondrocytes (35) that showed an increase in expression similar to that of p57 in mutant mice (Figure 5C). Similar up-regulation was observed for HIF-1α (Figure 5D), a sensor for low oxygen tension (36,37) that has been implicated in cartilage development (38).

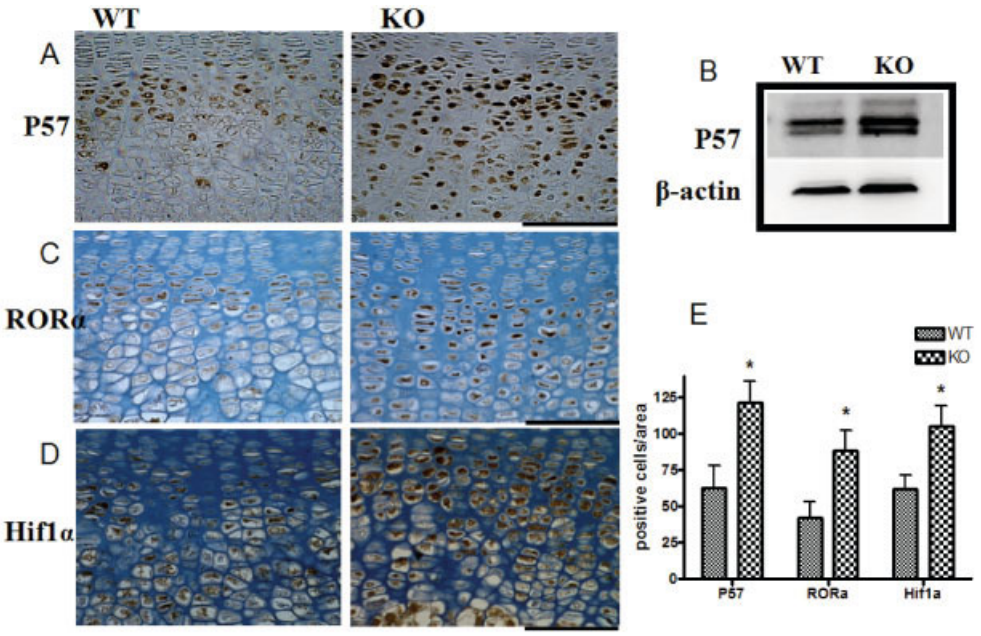

Figure 5. Premature differentiation of *eNOS*-deficient mouse chondrocytes. **A,** Increased expression of the cell cycle inhibitor protein p57 in knockout mice, as shown by immunohistochemistry. **B,** Western blot confirming increased expression of p57 in knockout mice. **C** and **D,** Up-regulation of the expression of the prehypertrophic and hypertrophic markers retinoic acid–related orphan receptor α (RORα) (**C**) and hypoxia-inducible factor 1α (HIF-1α) (**D**) in the growth plates of knockout mice, as shown by immunohistochemistry. Bars in **A, C,** and **D** = 200 μm. Results are representative of $\geq$4 experiments. **E,** Numbers of p57-positive, RORα-positive, and HIF-1α–positive cells per area, confirming the changes in the knockout mice. Bars show the mean and SD. $* = P < 0.05$ versus wild-type mice. See Figure 1 for other definitions.

Changes in cartilage-specific gene expression upon loss of *eNOS*. We sought to complement our immunohistochemistry results by quantitative analyses of gene expression, using real-time RT-PCR of RNA directly extracted from cartilage. Our results revealed decreased expression of the early chondrocyte markers *Col2a1* and *Sox9* and increased expression of the prehypertrophic markers *RORa* and *Hif1a* (Figure 6). In contrast, transcript levels for *Col10a1*, a marker of fully hypertrophic chondrocytes, were elevated only slightly (not significantly) in mutant mouse cells. These data suggest that the major phenotype in *eNOS*-deficient growth plates is the premature exit from the cell cycle and earlier prehypertrophic differentiation, with fewer effects on terminal differentiation.

DISCUSSION

While NO has been shown to play an important role in controlling chondrocyte physiology in OA, the roles of the 3 NO-synthesizing enzymes in cartilage development are less clear. In this study, we provide evidence for an important function of eNOS in the regulation of chondrocyte proliferation and differentiation. Our data show that genetic ablation of the *eNOS* gene in vivo results in reduced chondrocyte proliferation and endochondral bone growth. Analyses of the underlying molecular mechanisms suggest that these effects are likely due to altered expression of several cell cycle proteins and the modulation of intracellular pathways with known roles in chondrocyte differentiation, including *Sox9* and *Hif1*α.

Although there were no gross morphologic changes in the axial and appendicular skeleton of mutant mice, staining confirmed smaller rib cages, skull, and spine and shorter long bones. Some knockout mice showed more pronounced growth retardation and other defects such as kinky tails. The reasons for the variability in the phenotype are not known, but are consistent with the results of previous studies (22). Mice deficient in eNOS share some similarities with mice that lack C-type natriuretic peptide (CNP) (39), especially dwarfism and a reduction in chondrocyte proliferation. Because both

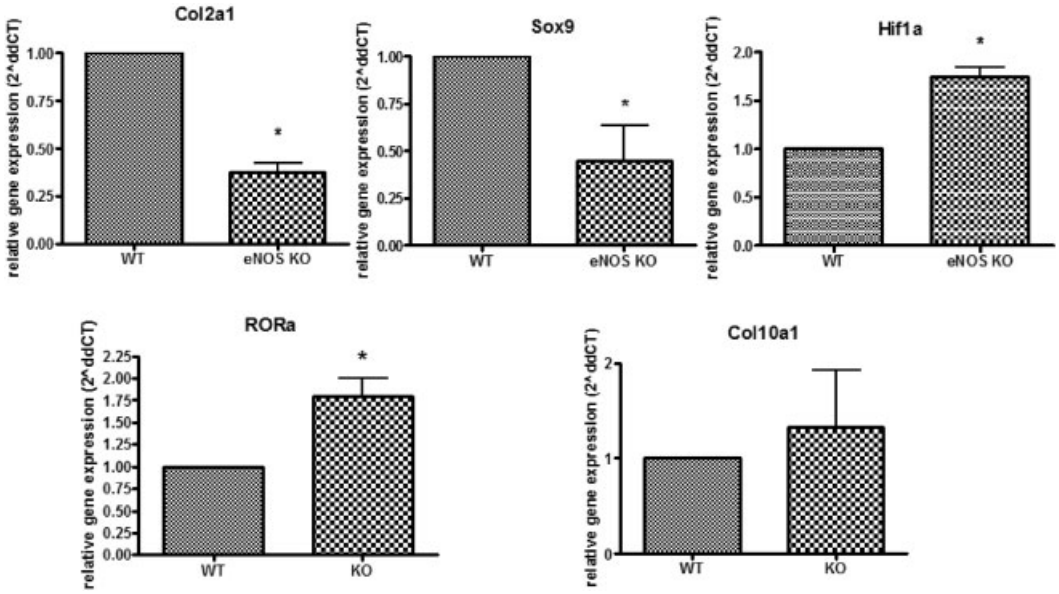

Figure 6. Promotion of prehypertrophic gene expression by *eNOS* deficiency. Real-time reverse transcriptase–polymerase chain reaction analyses using RNA extracted directly from neonate cartilage revealed decreased expression of the early chondrocyte markers *Col2a1* and *Sox9*, and increased expression of the prehypertrophic markers *RORa* and *Hif1a* in the cartilage of *eNOS*-knockout mice. Expression of the hypertrophic marker *Col10a1* was not significantly changed. Bars show the mean and SD ($n \geq 4$ independent experiments per genotype). $* = P < 0.05$ versus wild-type mice. See Figure 1 for definitions.

NO and CNP stimulate the production of cGMP via soluble or particulate guanylyl cyclases (19), these similarities are not surprising and provide further evidence of the importance of cGMP signaling in endochondral bone formation. However, the phenotype of *eNOS*-null mice does not exactly resemble that of mice lacking CNP or the main effector of cGMP in cartilage, cGMP-dependent kinase II (40). For example, mice lacking CNP have strikingly narrow growth plates and shorter proliferating and hypertrophic zones (39), which we did not see in the *eNOS*-deficient mice used in the present study.

Because NO is produced through different NOS isoforms, deletion of eNOS alone might be compensated for by the other 2 NOS enzymes. Indeed, we found a 2-fold up-regulation of nNOS transcript levels in *eNOS*-deficient mice, suggesting that these 2 constitutive forms have partially redundant roles in cartilage. Additionally, cGMP is not the only downstream target of NO; for example, NO can alter the activity of several proteins through tyrosine nitrosylation (41,42), which could account for some of the observed differences between *eNOS*-deficient mice and CNP- and cGMP-dependent kinase II–deficient mice.

A requirement of eNOS for proliferation has been described for a number of cells, including endothelial cells and osteoblasts (43,44). However, Teixeira and colleagues (20) demonstrated that NO signaling stimulates chondrocyte hypertrophy in chicken chondrocytes, raising the question of whether loss of eNOS promotes proliferation at the expense of differentiation or results in the opposite phenotype, e.g., reduced proliferation and earlier onset of maturation. Our results clearly support the latter model. While species-specific effects or differences in approaches (e.g., in vivo versus in vitro) could explain some of the differences between the results of our study and the results of the study by Teixeira (20), the more likely explanation is that NO effects in chondrocytes are differentiation stage and concentration dependent. For example, it is plausible to speculate that loss of only 1 NO-synthesizing protein has different effects from the pharmacologic inhibition of all 3 proteins.

Inactivation of eNOS results in reduced chondrocyte proliferation in vivo and in vitro. Considering that eNOS was deleted in all of the cells of the body in the mice used in this study, it was unclear whether the reduced chondrocyte proliferation was due to loss of

eNOS in cartilage or was secondary to defects in other tissues (e.g., in endocrine tissues or endothelial cells). Therefore, we conducted organ culture and primary cell culture in vitro, thus removing systemic and endocrine influences. Our organ culture data demonstrated reduced tibia growth upon loss of eNOS, and chondrocytes from mutant mice showed reduced multiplication of cells in culture. While these culture systems contain perichondral and periosteal cells that might be responsible for some of the observed changes, these results are consistent with the in vivo phenotype of *eNOS*-knockout mice and a cell-autonomous role of eNOS in chondrocyte proliferation.

The progression of the eukaryotic cell cycle is controlled by cyclins and cyclin-dependent kinases (32). For example, cyclin D1 has been shown to regulate the G_1 phase of the cell cycle, is expressed specifically in the proliferating zone of growth plates, and is required for maximal chondrocyte proliferation in vivo and in vitro (32,33). Our data showed a decline in cyclin D1 and an increase in p57 expression, presumably resulting in slower cell cycle progression and early cell cycle exit upon loss of eNOS. The earlier cell cycle exit and resulting acceleration in the onset of prehypertrophic differentiation is also supported by increased expression of prehypertrophic markers such as RORα and HIF-1α, and by reduced expression of markers for proliferating chondrocytes, such as type II collagen and SOX9. Of note, growth plate zone measurements and analyses of type X collagen expression suggest that eNOS deficiency accelerates prehypertrophic differentiation without accompanying acceleration of terminal hypertrophic differentiation.

In summary, our data demonstrate a role of eNOS in chondrocyte proliferation and endochondral bone growth. Loss of eNOS affects numerous aspects of cartilage physiology, including chondrocyte proliferation and gene expression. Further investigations into the specific mechanisms involved will result in a better understanding of physiologic and pathologic ossification and the role of eNOS in arthritic diseases.

AUTHOR CONTRIBUTIONS

All authors were involved in drafting the article or revising it critically for important intellectual content, and all authors approved the final version to be published. Dr. Beier had full access to all of the data in the study and takes responsibility for the integrity of the data and the accuracy of the data analysis.

Study conception and design. Yan, Feng, Beier.

Acquisition of data. Yan.

Analysis and interpretation of data. Yan, Beier.

REFERENCES

1. Abramson SB. Nitric oxide in inflammation and pain associated with osteoarthritis. Arthritis Res Ther 2008;10 Suppl 2:S2.
2. Abramson SB. Osteoarthritis and nitric oxide. Osteoarthritis Cartilage 2008;16 Suppl 2:S15–20.
3. Van't Hof RJ, Ralston SH. Nitric oxide and bone. Immunology 2001;103:255–61.
4. Mungrue IN, Bredt DS, Stewart DJ, Husain M. From molecules to mammals: what's NOS got to do with it? Acta Physiol Scand 2003;179:123–35.
5. Appleton CT, Pitelka V, Henry J, Beier F. Global analyses of gene expression in early experimental osteoarthritis. Arthritis Rheum 2007;56:1854–68.
6. Drissi H, Zuscik M, Rosier R, O'Keefe R. Transcriptional regulation of chondrocyte maturation: potential involvement of transcription factors in OA pathogenesis. Mol Aspects Med 2005;26: 169–79.
7. Gauci SJ, Golub SB, Tutolo L, Little CB, Sims NA, Lee ER, et al. Modulating chondrocyte hypertrophy in growth plate and osteoarthritic cartilage. J Musculoskelet Neuronal Interact 2008;8: 308–10.
8. Karsenty G, Wagner EF. Reaching a genetic and molecular understanding of skeletal development. Dev Cell 2002;2:389–406.
9. Zelzer E, Olsen BR. The genetic basis for skeletal diseases. Nature 2003;423:343–8.
10. Wagner EF, Karsenty G. Genetic control of skeletal development. Curr Opin Genet Dev 2001;11:527–32.
11. Olsen BR. Genetic regulation of skeletal patterning, differentiation, and growth. Bone 1999;25:77–9.
12. Goldring MB, Tsuchimochi K, Ijiri K. The control of chondrogenesis. J Cell Biochem 2006;97:33–44.
13. Kronenberg HM. Developmental regulation of the growth plate. Nature 2003;423:332–6.
14. Mackie EJ, Ahmed YA, Tatarczuch L, Chen KS, Mirams M. Endochondral ossification: how cartilage is converted into bone in the developing skeleton. Int J Biochem Cell Biol 2008;40:46–62.
15. Hoffman LM, Weston AD, Underhill TM. Molecular mechanisms regulating chondroblast differentiation. J Bone Joint Surg Am 2003;85-A Suppl 2:124–32.
16. Stanton LA, Underhill TM, Beier F. MAP kinases in chondrocyte differentiation. Dev Biol 2003;263:165–75.
17. Olsen BR, Reginato AM, Wang W. Bone development. Annu Rev Cell Dev Biol 2000;16:191–220.
18. Okazaki K, Iwamoto Y. Matrix gene regulation in cartilage. Clin Calcium 2006;16:1213–9. In Japanese.
19. Teixeira CC, Agoston H, Beier F. Nitric oxide, C-type natriuretic peptide and cGMP as regulators of endochondral ossification. Dev Biol 2008;319:171–8.
20. Teixeira CC, Ischiropoulos H, Leboy PS, Adams SL, Shapiro IM. Nitric oxide-nitric oxide synthase regulates key maturational events during chondrocyte terminal differentiation. Bone 2005;37: 37–45.
21. Shesely EG, Maeda N, Kim HS, Desai KM, Krege JH, Laubach VE, et al. Elevated blood pressures in mice lacking endothelial nitric oxide synthase. Proc Natl Acad Sci U S A 1996;93:13176–81.
22. Hefler LA, Reyes CA, O'Brien WE, Gregg AR. Perinatal development of endothelial nitric oxide synthase-deficient mice. Biol Reprod 2001;64:666–73.
23. Wang G, Woods A, Agoston H, Ulici V, Glogauer M, Beier F. Genetic ablation of Rac1 in cartilage results in chondrodysplasia. Dev Biol 2007;306:612–23.
24. Ulici V, Hoenselaar KD, Agoston H, McErlain DD, Umoh J, Chakrabarti S, et al. The role of Akt1 in terminal stages of endochondral bone formation: angiogenesis and ossification. Bone 2009;45:1133–45.
25. Solomon LA, Li JR, Berube NG, Beier F. Loss of ATRX in

chondrocytes has minimal effects on skeletal development. PLoS One 2009;4:e7106.
26. James CG, Appleton CT, Ulici V, Underhill TM, Beier F. Microarray analyses of gene expression during chondrocyte differentiation identifies novel regulators of hypertrophy. Mol Biol Cell 2005;16:5316–33.
27. Halawani D, Mondeh R, Stanton LA, Beier F. p38 MAP kinase signaling is necessary for rat chondrosarcoma cell proliferation. Oncogene 2004;23:3726–31.
28. Wang G, Woods A, Sabari S, Pagnotta L, Stanton LA, Beier F. RhoA/ROCK signaling suppresses hypertrophic chondrocyte differentiation. J Biol Chem 2004;279:13205–14.
29. Agoston H, Khan S, James CG, Gillespie JR, Serra R, Stanton LA, et al. C-type natriuretic peptide regulates endochondral bone growth through p38 MAP kinase-dependent and -independent pathways. BMC Dev Biol 2007;7:18.
30. Ulici V, Hoenselaar KD, Gillespie JR, Beier F. The PI3K pathway regulates endochondral bone growth through control of hypertrophic chondrocyte differentiation. BMC Dev Biol 2008;8:40.
31. Woods A, Wang G, Beier F. RhoA/ROCK signaling regulates Sox9 expression and actin organization during chondrogenesis. J Biol Chem 2005;280:11626–34.
32. Beier F. Cell-cycle control and the cartilage growth plate. J Cell Physiol 2005;202:1–8.
33. Beier F, Ali Z, Mok D, Taylor AC, Leask T, Albanese C, et al. TGFβ and PTHrP control chondrocyte proliferation by activating cyclin D1 expression. Mol Biol Cell 2001;12:3852–63.
34. James CG, Woods A, Underhill TM, Beier F. The transcription factor ATF3 is upregulated during chondrocyte differentiation and represses cyclin D1 and A gene transcription. BMC Mol Biol 2006;7:30.
35. Woods A, James CG, Wang G, Dupuis H, Beier F. Control of chondrocyte gene expression by actin dynamics: a novel role of cholesterol/Rorα signaling in endochondral bone growth. J Cell Mol Med 2009;13:3497–516.
36. Hwang PM, Byrne DH, Kitos PA. Effects of molecular oxygen on chick limb bud chondrogenesis. Differentiation 1988;37:14–9.
37. Koshiji M, Huang LE. Dynamic balancing of the dual nature of HIF-1α for cell survival. Cell Cycle 2004;3:853–4.
38. Schipani E, Ryan HE, Didrickson S, Kobayashi T, Knight M, Johnson RS. Hypoxia in cartilage: HIF-1α is essential for chondrocyte growth arrest and survival. Genes Dev 2001;15:2865–76.
39. Chusho H, Tamura N, Ogawa Y, Yasoda A, Suda M, Miyazawa T, et al. Dwarfism and early death in mice lacking C-type natriuretic peptide. Proc Natl Acad Sci U S A 2001;98:4016–21.
40. Pfeifer A, Aszodi A, Seidler U, Ruth P, Hofmann F, Fassler R. Intestinal secretory defects and dwarfism in mice lacking cGMP-dependent protein kinase II. Science 1996;274:2082–6.
41. Foster MW, Hess DT, Stamler JS. Protein S-nitrosylation in health and disease: a current perspective. Trends Mol Med 2009;15: 391–404.
42. Hess DT, Matsumoto A, Kim SO, Marshall HE, Stamler JS. Protein S-nitrosylation: purview and parameters. Nat Rev Mol Cell Biol 2005;6:150–66.
43. Beier F, Lee RJ, Taylor AC, Pestell RG, LuValle P. Identification of the cyclin D1 gene as a target of activating transcription factor 2 in chondrocytes. Proc Natl Acad Sci U S A 1999;96:1433–8.
44. Aguirre J, Buttery L, O'Shaughnessy M, Afzal F, Fernandez de Marticorena I, Hukkanen M, et al. Endothelial nitric oxide synthase gene-deficient mice demonstrate marked retardation in postnatal bone formation, reduced bone volume, and defects in osteoblast maturation and activity. Am J Pathol 2001;158: 247–57.